

so that there is considerable scope for advances by both experimentalists and theoreticians. The development of monodisperse sources of single well-defined metal clusters is being actively pursued by numerous groups worldwide, and the eventual availability of such sources together with the use of many rather than just one spectroscopic technique will allow their geometries, electronic structures, and reactions to be determined without equivocation. There are distinct commercial applications for clusters and small particles as evidenced

by the production of ~ 10 kg per month of such materials for commercial evaluation.⁸²

We thank NATO for a collaborative research grant (No. 442/82) and SERC for financial support. We have appreciated the many helpful discussions with Drs. J. S. Tse, J. R. Morton, K. F. Preston, and R. Sutcliffe and thank Drs. D. Cox, A. Kaldor, and Rohlfing for communicating their results prior to publication.

(82) (a) Tasahi, A.; Saegusa, N.; Oda, M. *IEEE Trans Magn.* 1983, 19, 1731. (b) Oda, M.; Saegusa, N. *Jpn. J. Appl. Phys.*, in press.

Energy Redistribution in Unimolecular Ion Dissociations

IVAN POWIS

Department of Chemistry, University of Nottingham, Nottingham NG7 2RD, United Kingdom

Received August 15, 1986 (Revised Manuscript Received February 13, 1987)

Introduction

Observation of unimolecular dissociations of gas-phase ions will be familiar to anyone who has had occasion to examine fragmentation patterns in mass spectra. The fundamental significance of these molecular ion dissociations has long been recognized and investigated. In principle, such dissociations are no different than those of neutral species, yet quite apart from their intrinsic interest ions hold special attractions when we wish to investigate elementary reaction processes. Prominent among these is that for bound electronic states the intermolecular potential at long range is frequently dominated by well-understood electrostatic forces. Even in the absence of specific information, we thus can start with a plausible working model for the long-range interaction potential. More pragmatically, we can note the experimental convenience which arises from the interaction of charged particles with electrostatic and magnetic fields. This permits efficient detection of individual ions and the use of some otherwise novel techniques. Mass spectrometry is of course one such example. Another more specialized example is photoelectron-photoion coincidence (PEPICO) detection of ions. Quite generally, PEPICO techniques allow the preparation and observation of energy-selected and, indeed, state-selected ions.

The central role of reactant energy gives us a paradigm for the understanding of elementary reactions. As a molecule dissociates, the configuration of its constituent parts (nuclei plus electrons) changes: this is reflected in changes of the potential energy and the disposition of nonpotential energy (vibrations, etc.). Following the evolution of the energy distribution through a reaction is ideally tantamount to following the rearrangement of the individual atoms. While this

remains an unrealized goal, we can at least seek to examine the energy redistribution apparent in the products coming from an initially state-selected reactant. As will be seen, this is a realistic option with PEPICO experiments where translational energy distributions can be readily obtained.

Perhaps the reader will find the probing of dissociation lifetimes (i.e., rates) a more familiar tactic for the characterization of dissociation mechanisms. In principle, both the lifetime and energy distributions will depend on the detailed dynamics of dissociation, but in practice these two types of data can be complementary. This is most clearly seen in the context of those many reaction theories which postulate a transition state or critical region of system phase space through which the system passes as it evolves from reactants to products.¹⁻³ In such cases the transition state represents a point of no return, and the lifetime is therefore assumed to be determined prior to this point. Interactions among the various degrees of freedom, affecting the observed final energy distribution of the products, can, however, persist to greater separations. In extremis one can argue that product lifetime distributions are determined by short-range dynamics whereas product energy distributions reflect the long-range dynamics of the system. While such statements may be somewhat lacking in rigor, they nevertheless appear to have a degree of validity, certainly for some types of unimolecular ion dissociation.⁴

The following Account considers some of these issues by using results obtained for energy redistribution in the dissociation of moderate sized ions.

The PEPICO Technique

PEPICO methods were first introduced by Brehm⁵ and in slightly more versatile form by Eland and co-workers.⁶ There now exist two major variants of the

Ivan Powis was a student at Oxford University from where he gained his D.Phil. in 1978 for work carried out under the supervision of C. J. Danby. He subsequently held an E.P.A. Cephalosporin Junior Research Fellowship at Lincoln College, Oxford, before taking up his present position as Lecturer in Physical Chemistry at the University of Nottingham in 1983. He was awarded the 1982 Meldola medal of the Royal Society of Chemistry for his work on gas-phase ion dissociation reactions.

(1) Forst, W. *Theory of Unimolecular Reactions*; Academic: New York, 1973.

(2) Pechukas, P. *Annu. Rev. Phys. Chem.* 1981, 16, 159.

(3) Hase, W. L. *Acc. Chem. Res.* 1983, 16, 258.

(4) Klots, C. E. *J. Chem. Phys.* 1964, 41, 117.

(5) Brehm, B.; von Puttkamer, E. *Adv. Mass Spectrom.* 1967, 4, 591.

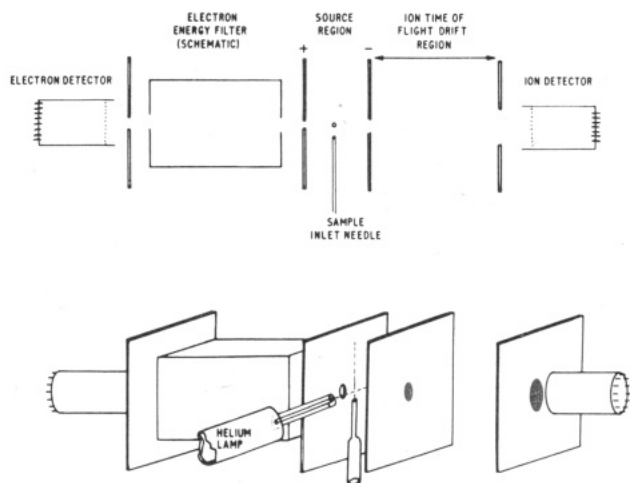


Figure 1. Schematic diagram showing plan and perspective views of a fixed-wavelength (resonance lamp source) PEPICO instrument.

technique which are compared and contrasted elsewhere.^{7,8} For the present Account a brief description of the author's experiment will suffice.⁹

Sample gas is admitted as an effusive jet into a vacuum chamber where some is ionized by an intersecting beam of UV light from a resonance lamp (Figure 1). Since a small electric field is impressed across the ionization region, the resulting electrons and ions are extracted in opposite directions. The electrons are energy-selected by passage through an electrostatic energy analyzer prior to their detection. When an ion and electron are detected simultaneously, i.e., in coincidence with one another, we recognize that they originated in the same ionization event. Moreover, we now know the initial energy of the ion because of simple considerations of energy balance: the initial energy of the (monochromatic) ionizing photon and the subsequent kinetic energy carried away by the electron are known, so that the difference has to be the energy deposited in the ionized molecule. Interpretation of the relevant photoelectron spectrum (PES) usually allows photoelectrons of a given kinetic energy to be associated with formation of a specific state of the accompanying parent molecular ion. Consequently, coincident ions can be electronic state selected. If vibrationally resolved PES are obtained, there is also vibrational state selection, but even without this we have an indication of the total vibrational energy of the selected state.

In practice, we do not expect exact coincidence between the two detector pulses. An allowance has to be made for the instrumental flight time of the ion, which will be modified if its mass changes en route to the detector due to fragmentation. The apparatus can therefore be operated as a time-of-flight (TOF) mass spectrometer in which the electron pulse establishes the precise moment of ion formation and starts the timing electronics. More subtly, if a fragment ion acquires extra velocity due to a release of excess energy in the dissociation, the flight time is again modified and can

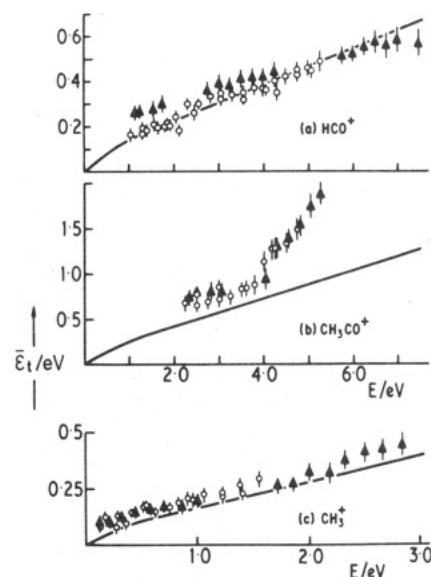


Figure 2. Mean translational energy, $\bar{\epsilon}_t$, as a function of excess energy, E , for dissociation of $C_2H_4O^+$ isomers (O, acetaldehyde; \blacktriangle , ethylene oxide) to the indicated products. Solid curves are from a statistical calculation.

be observed as a broadening of the fragment TOF peak shapes. From computer analysis of this broadening the center-of-mass (CM) energy released by dissociation of the state-selected parent can be found.

Energy Releases Conforming to a Statistical-Dynamical Model

We will now consider some results. Figure 2 shows mean CM kinetic energies ($\bar{\epsilon}_t$) for the three principal dissociation channels of acetaldehyde and isomeric ethylene oxide ions.¹⁰ These data points are presented as a function of the initial energy, E , in excess of the relevant dissociation threshold.

It is common to describe behavior of this type as "statistical". Ultimately, we will discuss this term more carefully, but some general observations explaining this choice can be made immediately. First, $\bar{\epsilon}_t$ increases smoothly as the excess energy increases and represents a small fraction of this excess, consistent with a statistical partitioning of energy among the internal degrees of freedom of the molecule prior to dissociation. More exactly, there is good agreement with the computed curves which assume equilibrium in the products.¹⁰ (Formation of CH_3CO^+ above 4 eV is evidently exceptional and is considered later.) Secondly, although these measurements were made in coincidence with photoelectrons from various bands of the PES, there is no evidence in Figure 2 of any dependence upon initial electronic state: rather, the total energy seems to be sufficient to characterize the observed behavior. Indeed, the behavior would seem to be independent of which isomeric form was ionized. Baer,¹¹ in particular, has studied many examples of isomeric systems among larger ions and frequently, though not exclusively, observed this independence. The inference drawn is that extensive rearrangement to a common form occurs in configuration space prior to dissociation. By implication there must then be extensive exploration of the energetically accessible system phase space giving rise

(6) Eland, J. H. D. *Int. J. Mass Spectrom. Ion Phys.* **1972**, *8*, 143.

(7) Dannacher, J.; Stadelmann, J.-P. *Spec. Period. Rep.: Mass Spectrom.* **1985**, *8*, 58.

(8) Baer, T. In *Gas Phase Ion Chemistry*; Bowers, M. T., Ed.; Academic: New York, 1979; Vol. 1.

(9) Powis, I.; Mansell, P. I.; Danby, C. J. *Int. J. Mass Spectrom. Ion Phys.* **1979**, *32*, 15.

(10) Johnson, K. M.; Powis, I.; Danby, C. J. *Chem. Phys.* **1982**, *70*, 329.

(11) Baer, T. *Adv. Chem. Phys.* **1986**, *64*, 111 and references therein.

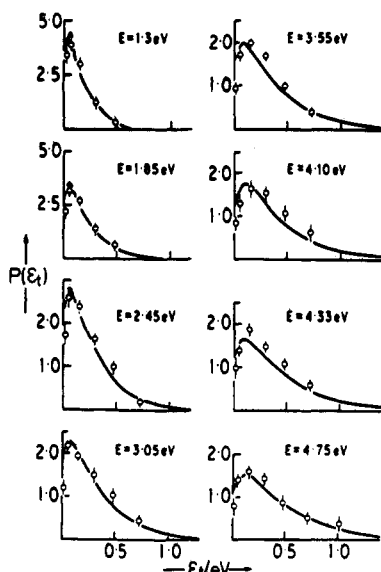


Figure 3. Examples of normalized KERDs, $P(\epsilon)$, for the dissociation $\text{CH}_3\text{CHO}^+ \rightarrow \text{HCO}^+ + \text{CH}_3$. The smooth curves are distributions calculated from a statistical-dynamical phase space theory.

to the energy "scrambling" postulated by statistical theories.

The mean energy is just the first moment of the associated probability distribution function, $P(\epsilon)$. One might expect this kinetic energy release distribution (KERD) to be more informative than the mean. Figure 3 shows some normalized KERDs for the first of the above fragmentations, $\text{CH}_3\text{CHO}^+ \rightarrow \text{HCO}^+ + \text{CH}_3$. All have the same qualitative appearance (a maximum at low energy followed by a quasi-exponential falloff) which has again come to be referred to as "statistical". The exponential tail of the KERD is readily understood in terms of a statistical hypothesis, for the probability of a given energy partitioning is related to the density of states, or phase space volume, available to accommodate that energy. As less energy is partitioned into translation, correspondingly more goes into vibration, and it is known that in the limit vibrational state densities increase approximately exponentially with energy.

Statistical phase space theory,^{12,13} in which a "loose" transition state (i.e., more akin to the products than reactants) is postulated, has proven to be particularly appropriate in this context. In order to both develop some understanding of the justification for the "loose" transition state and to explain the initial peaking of the KERD, we need, however, to consider the dynamics of dissociation.

The separation of ion and neutral fragments will take place under the influence of an effective potential which includes a repulsive centrifugal term arising from the orbiting motion of the two fragments

$$V_{\text{eff}}(r) = V(r) + L^2/2\mu r^2 \quad (\text{I})$$

where L is the orbiting angular momentum, μ the reduced mass, and r the separation. With an attractive true potential, $V(r)$, V_{eff} shows a maximum, the centrifugal barrier, at relatively large separation. At such distances the ion-induced dipole interaction may be taken to dominate the true potential so that $V(r) \approx$

$-\alpha e^2/2r^4$, where α is the neutral polarizability and e the charge. The validity and limitations of this approximation are well-established by the Langevin ion/molecule collision model;¹⁴ this related treatment for the reverse process of dissociation was first introduced by Klots.^{13,15}

The effect of the L -dependent centrifugal barrier is to impede dissociation when the radial kinetic (separation) energy is low, thereby reducing the observed probability of smaller energy releases. In considering the detail of centrifugal barrier effects, conservation of angular momentum must also be invoked and will restrict the allowable range of L (eq I). These dynamical considerations therefore introduce extra constraints to a simple statistical treatment.¹⁶⁻²⁰

It is now open to us to recognize the centrifugal barrier maximum as a "loose" transition state located at large separation distance and therefore possessing relatively well-defined productlike properties. For the calculation of rates this finds mixed success. Often a much "tighter" transition state seems to be called for,^{4,11} and recently there has been much speculation about the operation of alternative dynamically significant transition states lying within the centrifugal barrier.²¹⁻²³ For the calculation of KERDs, however, the statistical-dynamical approach is, not infrequently, remarkably successful. The form of computed KERDs around their maxima is found to be very sensitive to the dynamical constraints built into the model and to the assumed interaction potential. Examples of calculated KERDs are compared with experiment in Figure 3 to show the extent of the agreement attained. PEPICO experiments have revealed many other molecular ion dissociations where either good or excellent agreement can be claimed.^{10,16-18,24-32}

Molecular Rotations

The ability of PEPICO techniques to energy select the parent ion is limited not just by the apparatus resolution, which restricts our knowledge of the energy given to the ion on ionization, but also by uncertainty about the thermal energy already deposited in the neutral. In larger molecular ions the contribution from

- (14) Su, T.; Bowers, M. T. In ref 9.
 (15) Klots, C. E. *Z. Naturforsch., A: Phys., Phys. Chem., Kosmophys.* 1972, 27, 553; *J. Chem. Phys.* 1976, 64, 4269.
 (16) Powis, I.; Danby, C. J. *Chem. Phys. Lett.* 1979, 65, 390.
 (17) Powis, I. *J. Chem. Soc., Faraday Trans. 2* 1979, 75, 1294.
 (18) Powis, I. *J. Chem. Soc., Faraday Trans. 2* 1981, 77, 1433.
 (19) Chesnavich, W. J.; Bowers, M. T. *J. Am. Chem. Soc.* 1977, 99, 1706.
 (20) Johnson, K. M.; Powis, I.; Danby, C. J. *Chem. Phys.* 1981, 63, 1.
 (21) Chesnavich, W. J.; Bass, L. M.; Su, T.; Bowers, M. T. *J. Chem. Phys.* 1981, 74, 2228.
 (22) Dodd, J. A.; Golden, D. M.; Braumann, J. I. *J. Chem. Phys.* 1984, 80, 1894.
 (23) Truhlar, D. G. *J. Chem. Phys.* 1985, 82, 2166; Chesnavich, W. J.; Bowers, M. T. *Ibid.* 1985, 82, 2168.
 (24) Mansell, P. I.; Danby, C. J.; Powis, I. *J. Chem. Soc., Faraday Trans. 2* 1981, 77, 1449.
 (25) Powis, I. *Chem. Phys.* 1982, 68, 251.
 (26) Mintz, D. M.; Baer, T. *J. Chem. Phys.* 1976, 65, 2407.
 (27) Powis, I. *Chem. Phys.* 1983, 74, 421.
 (28) Lightfoot, P. D.; Powis, I.; Danby, C. J. *Chem. Phys. Lett.* 1983, 96, 232.
 (29) Ogden, I. K.; Shaw, N.; Danby, C. J.; Powis, I. *Int. J. Mass Spectrom. Ion Processes* 1983, 54, 41.
 (30) Low, K. G.; Hampton, P. D.; Powis, I. *Chem. Phys.* 1985, 100, 401.
 (31) Miller, B. E.; Baer, T. *Chem. Phys.* 1984, 85, 39.
 (32) Brand, W. A.; Baer, T.; Klots, C. E. *Chem. Phys.* 1983, 76, 111.

(12) Light, J. C. *Discuss. Faraday Soc.* 1967, 44, 14.

(13) Klots, C. E. *J. Phys. Chem.* 1971, 75, 1526.

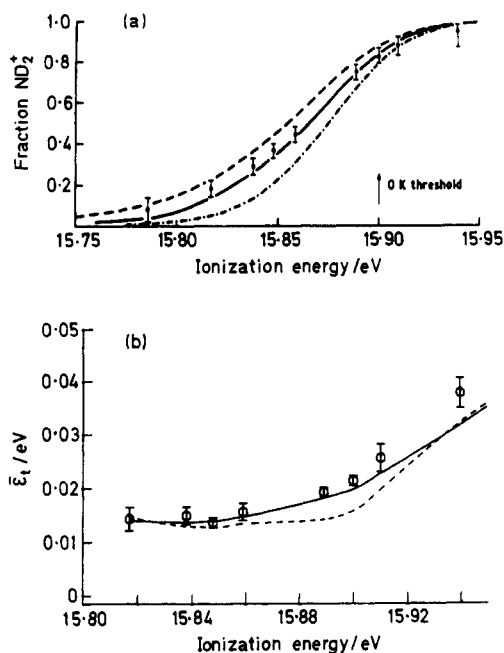


Figure 4. (a) Fractional abundance of ND_2^+ from ND_3^+ around the 0 K threshold for dissociation. Calculated curves assume all rotational energy is available for reaction at various temperatures: (---) 200 K (—) 300 K, and (- - -) 400 K. (b) Mean energy releases for this dissociation. The curves now are the predictions of a statistical-dynamical model both with (—) and without (---) correction for finite instrumental resolution.

thermal vibrational energy can be large and requires careful assessment,⁷ but for many of the smaller ions which we have examined it is usually possible to assume the vibrationally hot component is negligible. This then leaves the question of rotational energy to be considered.

In the statistical-dynamical approach rotations of both parent and molecular fragments feature prominently as sources of angular momentum to be conserved. Moreover, it is implicit in the phase space evaluation that, subject to the acknowledged constraints, rotational degrees of freedom are fully involved. Evidence for the free availability of parent rotational energy in ion dissociations can be found in the observed temperature dependence of near-threshold dissociative photoionization of CH_4^+ ³³ and NH_3^+ .³⁴ This is confirmed indirectly by the analysis of PEPICO experiments for several molecules including CH_4^+ ¹⁷ and, more directly, by PEPICO data obtained at ionization energies around the 0 K threshold for H loss by NH_3^+ .^{18,25} Below this threshold only thermally hot ions have sufficient energy to fragment, and because of high vibrational frequencies, such energy is predominantly rotational in origin. Figure 4a shows the fractional yield of ND_2^+ around threshold; this behaves exactly as would be expected if rotational energy were freely available.

The mean energy releases measured for this fragmentation are shown in Figure 4b. What is immediately interesting about these ND_2^+ data is that they do not extrapolate to zero as one approaches lower ionization energy but rather achieve a limiting value,²⁵ and for NH_2^+ they actually increase.¹⁸ The explanation can be found by examination with the statistical-dynamical model which behaves likewise. Below the 0 K threshold

the fragmenting sample is increasingly comprised of rotationally hot ions, and the mean angular momentum of the dissociating systems necessarily increases. Quite generally, this suggests the involvement of larger "L" centrifugal barriers: this is especially true for these particular products which, due to exceptionally large rotational constants, cannot, on energetic grounds, readily accommodate much of the total angular momentum as product rotation. Hence, the constraints of the centrifugal barrier are pronounced and so strongly disfavor partitionings with small translational energy. The quantitative success in modeling these $\text{NH}(\text{D})_3^+$ data offers an indication of the aptness not only of the statistical-dynamical formulation, but more specifically of the assumed r^{-4} potential.

Scaling Properties of the KERDs

Full evaluation of the information contained in a complete set of KERDs poses certain difficulties, in that it is hard to assimilate all the data. (Recall Figure 3 shows just a few examples of the KERDs available for that one dissociation channel.) In an effort to overcome this problem, we have remarked on the phenomenological property of such statistical KERDs to scale:²⁰ that is to say that when appropriately renormalized KERDs are plotted as a function of a reduced energy parameter (e.g., $f_t = \epsilon_t/E$), they have quantitatively the same form over a range of values of E . This has been experimentally verified for a number of ions including those of methane,¹⁷ acetone,²⁰ various alkyl halides,^{26,27,31,32} and MeNO_2 ²⁹ and is also found to be true of statistically computed KERDs.^{20,32}

Scaling the KERDs helps to compact large amounts of data and facilitates comparison with theoretical models. Additionally, any deviations from scaling behavior may be indicative of changes in the dissociation dynamics. A rather obvious illustration of this is found in the results for CH_3CO^+ formation presented previously.¹⁰ Above a certain threshold the slope of the mean energy plot, Figure 2b, changes, and the associated KERDs indicate a diminished probability for the observation of small energies. This is attributable to a "loss" of low kinetic energy ions through the secondary dissociation $\text{CH}_3\text{CO}^+ \rightarrow \text{CHO}^+$. Analogous behavior is found for $\text{MeNO}_2^+ \rightarrow \text{NO}_2^+ \rightarrow \text{NO}^+$.²⁹ Primary fragments having rather little energy partitioned into their relative translation will contain correspondingly more energy in internal modes, and they consequently have a greater propensity for further dissociation. More subtle uses of scaling to elucidate dissociation behavior may be found in the reactions $\text{MeI}^+ \rightarrow \text{Me}^+$ ²⁷ and $\text{EtBr}^+ \rightarrow \text{Et}^+$.³¹

Validity of Statistical Energy Distributions

The introduction of statistical hypotheses into a theoretical treatment is usually necessitated by the lack of any more specific knowledge; i.e., it acknowledges a condition of "maximum ignorance". In one respect it therefore offers a yardstick of comparison against which to seek "more interesting" nonstatistical behavior. Yet to use the appellation "statistical" in a casual and perhaps dismissive sense is to run the risk of overlooking many features of interest. Often behavior is loosely called statistical to indicate some degree of qualitative conformance with statistical expectations. Yet we remark on the frequency with which good

(33) McCulloh, K. E.; Dibeler, V. H. *J. Chem. Phys.* **1976**, *64*, 4445.

(34) McCulloh, K. E. *Int. J. Mass Spectrom. Ion Phys.* **1976**, *21*, 333.

quantitative agreement can be obtained for the KERDs in ion dissociations, providing the statistical assumptions are carefully defined and that centrifugal barrier and angular momentum constraints are properly allowed for. This is not to suggest that all ion dissociations are statistical (far from it) but that for those reactions which can be presumed to take place on quasi-bound surfaces a statistical-dynamical model can be surprisingly successful in describing product energy distributions.

Fully statistical behavior would imply statistical branching into all thermodynamically accessible channels and that all concurrent channels were statistical in nature. Yet, for example, the dissociation of the second excited electronic state of MeI^+ yields Me^+ and I^+ with "statistical" energy release, but simultaneously CH_2I^+ with a very large "nonstatistical" release.²⁷ Apparently, here there is complex behavior which involves dissociation over several surfaces. More generally, there are many instances where certain electronic states of a given ion dissociate with statistical KERDs, while others do not; examples include CF_3X^+ ,^{30,35} NF_3^+ ,²⁴ and EtBr^+ .³¹ In yet other cases (e.g., MeI^+ ,²⁷ MeNO_2^+ ²⁹) a nonstatistical preference for the production of an excited-state product is perhaps found. Electronically state specific behavior is evidently common with these moderately sized ions. That there should be an electronic state dependence is not really surprising. We have, however, to introduce it as another constraint when evaluating accessible phase space and should therefore refer more precisely to the frequent successes of the statistical-dynamical model as instances of electronically specific, but vibrationally and rotationally ergodic, behavior.

Why then should a statistical distribution of product kinetic energy (if not necessarily of lifetimes) be so often observed? In some measure this may be due to the aptness, at long range, of the ion-induced dipole potential and the ensuing centrifugal barrier, which is thus largely independent of specific details of the true, short-range potential. Within the barrier the dynamics can be complex, but once at the barrier the partitioning between kinetic and nonkinetic product energy is finally defined and simply modeled. This last statement somewhat glosses over questions concerning whether the distribution of nonkinetic energy is statistical, for which there is currently little direct experimental data, but some interesting insights in this respect have been emerging from a series of ab initio studies of ion dissociations.³⁶ These calculations have stressed the importance of nonadiabatic interactions, and especially the role played by conical intersections between electronic states. Such localized interactions arise around the crossing of two nondegenerate states of different symmetry. Excitation of a mode which removes an element of symmetry may cause both states to belong to the same representation in the lowered symmetry and so to repel one another. The resulting surfaces in two-dimensional space resemble two cones touching at their apex.

An example where nonadiabatic interactions have been well studied can be found in the ion C_2H_4^+ .³⁷⁻³⁹

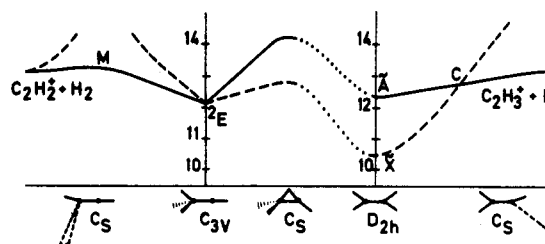


Figure 5. Folding screen representation of $\text{C}_2\text{H}_4^+ \rightarrow \text{C}_2\text{H}_2^+$ reaction path. Point C is the conical intersection between the \tilde{A}^2A' and \tilde{X}^2A'' surfaces. Taken from Lorquet, ref 39.

Figure 5 shows a reaction path for the H_2 elimination reaction as deduced by Lorquet.³⁹ Simple 1,2-elimination by the \tilde{A} state ion entails a large energy barrier and is apparently precluded by the experimental observation of vanishingly small translational energy releases.²⁸ Instead, the following sequence can be proposed: C-H bond extension to reach the conical intersection "C"; rapid conversion to the \tilde{X} state surface at this intersection; H atom migration via a C_s bridged structure to give $\text{CH}_3\text{-CH}^+$; passage through this C_{3v} Jahn-Teller state to the product via a 1,1- H_2 elimination. This final dissociation step has no, or only a minimal, barrier and so is consistent with the experimental data. The implications of this somewhat tortuous route for energy randomization are as follows: the symmetric modes initially excited in photoionization must be coupled to nonsymmetric stretches to achieve the configuration "C"; a torque is exerted at the conical intersection which can excite the torsional mode; attaining the bridged structure requires involvement of bending modes; finally, excitation of an e mode is induced by passage through the degenerate Jahn-Teller state. In short, all 12 vibrational modes of this ion have been invoked in following the suggested reaction path. Lorquet's suggestion³⁹ is thus that for the system to wind its way through a rather specific but necessary route to the final products, in which a great variety of configurations are adopted, fairly extensive redistribution of energy through the vibrational modes is inevitable.

It remains to be established how general this picture will prove, although similar treatments have been made for other small ion dissociations.³⁶ Conical intersections are known to figure in the dynamics of neutral reaction systems but may prove to play an even more prominent role in ions. Adjacent states in open-shell ions typically differ in configuration by only one electron, and the coupling matrix elements will then be large as the coupling is a single particle effect. In contrast, neighboring states in closed-shell species may differ by more than one electron with vibronic coupling then occurring only through configuration interaction.³⁸ Less fundamentally, ions tend to be "floppier" than neutrals so are generally likely to explore more of their configuration space and hence are more likely to encounter dynamically significant regions of interaction. For bigger ions of greater dimensionality such pathways may be so likely as to be the norm. This would certainly account

(35) Powis, I. *Mol. Phys.* 1980, 39, 311.

(36) Desouter-Lecomte, M.; Dehareng, D.; Leyh-Nihant, B.; Praet, M. Th.; Lorquet, A. J.; Lorquet, J. C. *J. Phys. Chem.* 1985, 89, 214 and references therein.

(37) Köppel, H.; Cederbaum, L. S.; Domcke, W. *J. Chem. Phys.* 1982, 77, 2014.

(38) Köppel, H. *Chem. Phys.* 1983, 77, 359.

(39) Sannen, C.; Raseev, G.; Galloy, C.; Fauville, G.; Lorquet, J. C. *J. Chem. Phys.* 1981, 74, 2402.

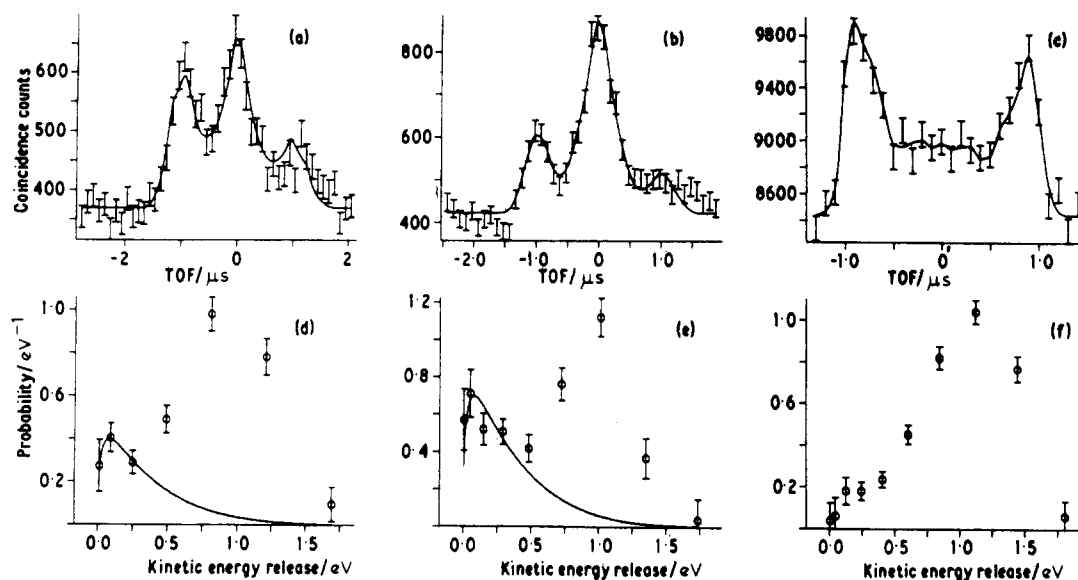


Figure 6. \tilde{A}^2A_1 $CF_3Cl^+ \rightarrow CF_3^+$ TOF peaks under the following conditions: (a) 15.1-eV ionization energy, He I radiation; (b) 15.4 eV, He I; (c) 15.4 eV, Ne I radiation. Beneath are the experimental KERDs (as points) and statistical-dynamical calculations (curves).

for the commonly observed phenomenon whereby larger ions isomerize and relax to the ground electronic state prior to dissociation.

State vs. Energy Selection

In the foregoing presentation of PEPICO results it has been tacitly assumed that electron energy selection does achieve ion state selection. If that were so, then the data should be independent of the specifics of the ionization process. In general, this indeed borne out by experience, but there are some instances where different behavior is noted, notably when data recorded with resonance lamps for ionization are compared with results obtained at the same nominal ionization energy but with threshold ionizing wavelengths.^{40,41} Evidently, in such cases determination of the ionization energy via the selected electron energy is not sufficient to characterize completely the ion which is prepared.

Occasionally, differences may also be observed according to whether a He or Ne resonance lamp is employed.³⁵ Figure 6 shows CF_3^+ TOF peaks recorded following the preparation of (nominally) \tilde{A}^2A_1 CF_3Cl^+ . With a Ne lamp a broad peak (dished in appearance due to instrumental discrimination effects) is observed, indicating a large energy release. The detailed KERD confirms this and suggests an essentially direct dissociation on a repulsive surface. When instead He I radiation is used, a much narrower peak appears, superimposed on the original broad one. The now bimodal KERD appears no different at large translational energies but shows an additional low-energy release channel, reminiscent of the "statistical" dissociation of the ground state.¹⁶ A plausible explanation is that some ions are formed in a vibrationally hot ground state degenerate with the intended \tilde{A} state, presumably through some accidental autoionization at the He I wavelength. In the future systematic investigations of the precise role of differing ionization routes on the

dissociative behavior of ions may be expected to yield considerable insight into the dynamics of dissociative photoionization.

Anisotropy in Dissociative Photoionization

A second assumption which has been made more or less tacitly in most analyses of TOF peak shapes is that the observed fragmentation is isotropic in the Lab frame. This is an important assumption if one wishes to extract information concerning energy distributions from a single TOF peak as simultaneous deconvolution of an unknown angular distribution cannot possibly yield a unique result. While there is currently little reason generally to jettison this assumption, Eland⁴² has attributed asymmetric peak shapes recorded with NO^+ to anisotropic fragment distributions. Recently, we have found a dramatic and clear demonstration of such effects with CF_3I^+ .³⁰

The \tilde{A} state of this ion can dissociate to both I^+ and CF_3^+ , and indeed both are observed (Figure 7). However, both show TOF peak shapes which are distorted from what is expected for isotropically distributed fragments and, significantly, the asymmetric distortions are in opposite senses. The I^+ peak has an intensity distribution suggesting that I^+ fragments are initially projected preferentially backward in the apparatus and the CF_3^+ projected preferentially forward toward the ion detector.

How can this arise? There will of course be some photoionization anisotropy associated with the anisotropy of the ionizing light beam, but this is of limited importance here. More importantly, it can be noted that the geometry of the apparatus will necessarily tend to discriminate against and disfavor the observation of ions and, more especially, electrons unless they are emitted in certain directions in the Lab frame. The coincidence detection scheme thus establishes not just the temporal correlation between electron and ion fragments, but also a correlation between the directions of these particles. To be prosaic, only if the photoelectron is ejected toward the electron detector will it

(40) Nenner, I.; Guyon, P.-M.; Baer, T.; Govers, T. R. *J. Chem. Phys.* 1980, 72, 6587.

(41) Richard-Viard, M.; Dutuit, O.; Amarkhodja, A.; Guyon, P.-M. In *Photophysics and Photochemistry above 6eV*; Lahmani, F., Ed.; Elsevier: Amsterdam, 1985.

(42) Eland, J. H. D. *J. Chem. Phys.* 1979, 70, 2926.

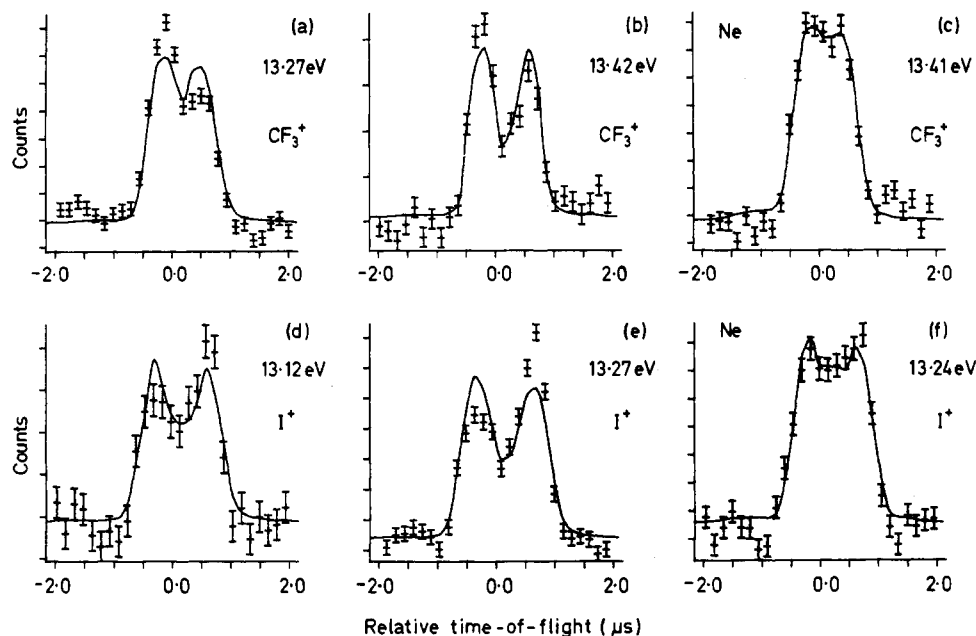


Figure 7. Examples of coincidence TOF peaks from \tilde{A}^2A_1 CF_3I^+ : (a),(b) CF_3^+ with He I radiation; (c) CF_3^+ , Ne I radiation; (d),(e) I^+ , He I; (f) I^+ , Ne I. Nominal ionization energies as shown. The curves through the data are computed best-fit *isotropic* distributions.

be observed. If, moreover, the photoionization dynamics yield a photoelectron angular distribution which is strongly peaked in the *molecular* coordinate frame, then only that subset of the randomly oriented gas-phase sample which happens to be "facing" the right way will eject electrons toward their detector; thus, the only ions to be detected in coincidence with electrons will come from appropriately oriented molecules. It does indeed appear that CF_3I^+ must release electrons very preferentially along the C→I bond direction to give a strong orientation to those ions seen in coincidence with electrons. If finally we make the apparently justifiable assumption³⁰ that C–I bond cleavage is rapid, in fact that it occurs under axial recoil conditions, then we have an explanation for the observed CF_3 and I peak shape anomalies, for then the fragment ion directions will be indicative of the orientation of the molecular axis at the moment of ionization.

Useful corroboration of the above explanation comes from repeating the experiments with lower energy photons when the photoelectron energy is correspondingly reduced. The angular discrimination against electrons is then lessened by the increased effectiveness of the source field in sweeping up all electrons into the right direction. This gave qualitatively very different looking, more symmetric TOF peak shapes when Ne rather than He radiation was used (Figure 7), as expected.³⁰

The above discussion shows how one can obtain orientation effects in PEPICO experiments when both electron and fragment ion directions are strongly correlated through the molecular frame. When only one particle shows a strong dependence on the molecular coordinates, its direction could nevertheless be used to indicate the orientation of the molecule as it is ionized.

This could then allow for the angular distribution of the other fragment relative to the molecular rather than Lab frame to be determined. It just so happens that many of the dissociations studied to date have been relatively long lived predissociations in which such effects are "washed out" below the limits of detectability by the effects of molecular rotation.

Conclusions

In this Account the use of PEPICO techniques to measure the distribution of translational energy accompanying the unimolecular dissociation of state-selected ions has been outlined. Results of "statistical" type reactions have been highlighted, and a picture of electronically state specific but vibrationally and rotationally ergodic behavior emerges. Angular momentum related effects play a distinct role, and though the systems are quite sensitive to this, a simple dynamical treatment is surprisingly effective. In considering why a statistical–dynamical model may be so frequently appropriate, the importance of nonadiabatic interactions is suggested, and it seems likely that this will provide a focus for future investigations. The development of new methods for the state-selective preparation of ions, such as resonance-enhanced multiphoton ionization, seems likely to give added impetus to this work. At the same time it seems inevitable that one will in future wish to consider the dynamics of dissociative photoionization per se as our awareness of the interplay of different electronic states and the dependence upon the photoionization route adopted grows.

It is a pleasure to acknowledge the contributions of students and colleagues to this work. In particular, I thank Drs. K. M. Johnson and C. J. Danby for many valuable discussions, ideas, and assistance.